

Relationship between the thermal properties and degree of saturation of cementitious grouts used in vertical borehole heat exchangers

Daehoon Kim, Seokhoon Oh*

Energy & Resources Engineering, Kangwon Nat'l University, Gangwondaehak-Gil 1, Kangwon-do, Chuncheon 24341, Republic of Korea

ARTICLE INFO

Article history:

Received 19 February 2019

Revised 26 June 2019

Accepted 8 July 2019

Available online 8 July 2019

Keywords:

Vertical borehole heat exchanger

Thermal conductivity

Cementitious grout

Specific-heat capacity

ABSTRACT

Although the thermal properties of soil and rock are strongly affected by moisture content, a number of previous experimental studies on the grouting materials used in vertical borehole heat exchangers (BHEs) have assessed their thermal properties under saturated and dried conditions. These studies have focused primarily on measurement and improvement of thermal conductivity. However, recent numerical studies on vertical BHEs reported that when a vertical BHE is under intermittent operation both the thermal conductivity of the grouting material and its high specific-heat capacity have a positive effect on the performance of the BHE. Moreover, because both the specific-heat capacity and thermal conductivity of the grouting material are essential parameters when numerically simulating vertical BHEs, they should be investigated together. In this study, cementitious grout specimens were prepared for use in vertical BHEs with different water/cement (w/c) and sand/cement (s/c) ratios, and their thermal conductivity and specific-heat capacity under saturated, air-dried, and partially saturated conditions were measured. Furthermore, the relationships of the mixing ratio of cementitious grout, degree of saturation, and thermal properties were analyzed. The thermal conductivity and specific-heat capacity of cementitious grout decreased by 15.56–38.30% and 11.79–22.34%, respectively, under air-dried rather than saturated conditions. Moreover, under partially saturated conditions, the thermal conductivity and specific-heat capacity of cementitious grout decreased linearly with the degree of saturation. The thermal conductivity of the cementitious grout was more significantly affected by variations in the s/c ratio than in the w/c ratio, while the specific-heat capacity was affected by the amount of water in voids. The results were used to derive empirical equations to predict the thermal properties of cementitious grouts with various mixing ratios, which are expected to be useful for further studies on vertical BHEs.

© 2019 Elsevier B.V. All rights reserved.

1. Introduction

Heating, ventilation, and air conditioning (HVAC) systems are the primary sources of energy consumption in residential and commercial buildings. In 2017, the residential and commercial sectors used approximately 39% of the total energy consumed in the United States [1,2]. In addition, in spite of the international requirements for reducing greenhouse gas emissions, residential and commercial buildings are large contributors to carbon dioxide (CO₂) emissions [3]. Therefore, various attempts have been made to reduce greenhouse gas emissions and optimize the energy consumption of HVAC systems. [4–8]. Among HVAC technologies, ground source heat pump (GSHP) systems are the most energy-efficient examples currently on the market [9].

GSHP systems are preferred as alternative-energy systems because they use heat energy from the Earth, which is both environ-

mentally friendly and inexhaustible. Notably, the US Environmental Protection Agency (EPA) reported that GSHP systems are the most energy-efficient, clean and cost-effective space-conditioning systems available [10]. GSHP systems use the ground as a heat sink for cooling, or as a heat source for heating. Worldwide, most GSHP systems use vertical borehole heat exchangers (BHEs), which usually offer higher energy performance due to the lower temperature fluctuations in the ground [11,12]. When a vertical BHE is installed, a borehole with a diameter of 0.1–0.3 m and a depth of 50–200 m is drilled into the ground [13]. Afterwards, a U-tube high-density polyethylene (HDPE) pipe is placed in the borehole. The borehole is then filled with grouting materials, such as bentonite or cement (Fig. 1). Because vertical BHEs exchange heat with the surrounding ground by circulating a fluid, such as pure water or antifreeze, through the U-tube HDPE pipe, the grouting materials in the borehole should have high thermal conductivity to facilitate efficient heat transfer between the BHE and the surrounding ground. However, pure grouting materials such as cement and water and bentonite and water mixes have relatively low thermal

* Corresponding author.

E-mail address: gimul@kangwon.ac.kr (S. Oh).

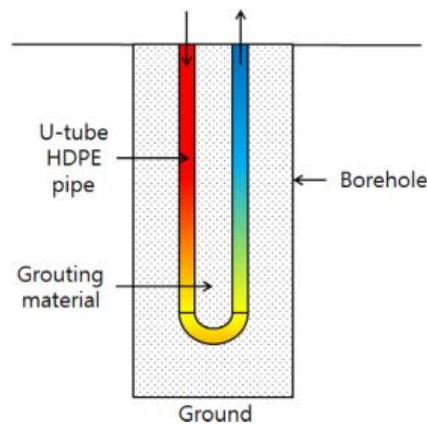


Fig. 1. Schematic diagram of a vertical borehole heat exchanger (BHE) with a U-tube high-density polyethylene (HDPE) pipe.

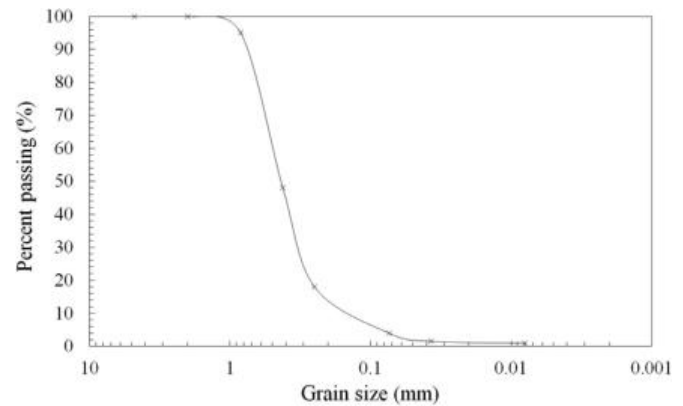


Fig. 2. Grain-size distribution curve of natural silica sand.

conductivity, which is unfavorable for heat transfer [14]. Hence, various studies have been carried out to address this problem.

Remund and Lund [15] measured the thermal conductivity of bentonite grouts mixed with various additives (masonry sand, limestone, quartzite etc.), and reported that most of the additives increased thermal conductivity by up to 100%. Omer [16] carried out laboratory tests to evaluate the thermal conductivity of bentonite grouts with additives of fine or coarse sand and reported an optimal percentage of bentonite in the dry mass of 10–12%. Lee et al. [17] prepared seven types of bentonite grouts using silica sand or graphite as additives and evaluated their thermal conductivity and viscosity. They found that while thermal conductivity rose with increasing additive content, viscosity also increased.

One of the problems with bentonite grouts is that they are susceptible to shrinkage and cracking due to moisture loss [18]. Therefore, they have gradually been replaced with cementitious grouts, which are relatively inexpensive and easy to work [19,20]; their properties have been well characterized.

To confirm the overall applicability of cementitious grouts, Park et al. [21] prepared cementitious grouts with various mix proportions and investigated their thermal conductivity, unconfined compression strength, and equivalent hydraulic conductivity. Allan and Kavanaugh [20] measured the thermal conductivity of cementitious grout and bentonite grout using silica sand as an additive and reported that cementitious grout had higher thermal conductivity than bentonite grout. Allan and Philippacopoulos [22] evaluated the thermal, mechanical, and hydraulic properties of cementitious grouts, and developed a grout mix (MIX 111) containing silica sand. Altimiri and Rouainia [23] measured the thermal conductivity of cementitious grouts mixed with sand, flourspar, glass and pulverized fuel ash (PFA), and found that cementitious grout had high thermal conductivity when mixed with flourspar, coarse ground glass, and PFA.

Recent numerical studies on vertical BHEs reported that, in intermittent operation mode, increasing both the thermal conductivity and specific-heat capacity of the grouting material has a positive effect on the performance of vertical BHEs [24,25]. The system is in intermittent operation mode when it is switched on or off based on the heating or cooling demands of residential and commercial buildings. Vertical BHE systems are generally operated in this mode [26]. However, previous experimental studies have focused primarily on measurement and improvement of the thermal conductivity of grouting materials and ignored the specific-heat capacity. Also, the thermal properties of soil or rock are strongly affected by their moisture content [27–29]. Therefore, after a vertical GHE has been installed, fluctuations in the groundwater level,

rainfall infiltration, and evapotranspiration can affect the moisture content of both the grouting material and the surrounding ground, and by extension their thermal properties. However, the aforementioned previous experimental studies investigated the thermal conductivity of grouting materials only under saturated and dry conditions. Moreover, the effects of varying the moisture content on the thermal properties of grouting materials have rarely been investigated. The handful of studies that have investigated these effects have focused on thermal conductivity [30,31] and neglected specific-heat capacity. Furthermore, because both the thermal conductivity and specific-heat capacity of grouting materials are essential parameters for numerical simulations of vertical BHEs, they should be investigated together.

In this study, the thermal conductivity and specific-heat capacity of cementitious grouts used for vertical BHEs were investigated. Nine types of cementitious grout specimens with different water/cement (w/c) and sand/cement (s/c) ratios were prepared, and their thermal conductivity and specific-heat capacity were measured under saturated, air-dried, and partially saturated conditions. The relationships of the mixing ratio of cementitious grouts, degree of saturation, and thermal properties were also analyzed. The results were then applied to derive empirical equations for the thermal properties of cementitious grouts with various mixing ratios.

2. Materials and methods

2.1. Mix proportions and specimen preparation

The cement used in this study was ordinary Portland cement (ASTM TAYPE I). Natural silica sand was used as an additive to increase the thermal conductivity of the cementitious grout, and its grain size distribution is plotted in Fig. 2. Nine mix proportions of cementitious grouts, with different (w/c) and (s/c) ratios, were tested, as used in previous studies [25]. These are listed in Table 1. For each mix proportion, three cylindrical specimens were

Table 1

Mix proportions of the cementitious grout specimens.

Specimen no.	Water/Cement ratio	Sand/Cement ratio
WC03-SC00	0.3	0
WC03-SC05	0.3	0.5
WC03-SC10	0.3	1
WC04-SC00	0.4	0
WC04-SC05	0.4	0.5
WC04-SC10	0.4	1
WC05-SC00	0.5	0
WC05-SC05	0.5	0.5
WC05-SC10	0.5	1

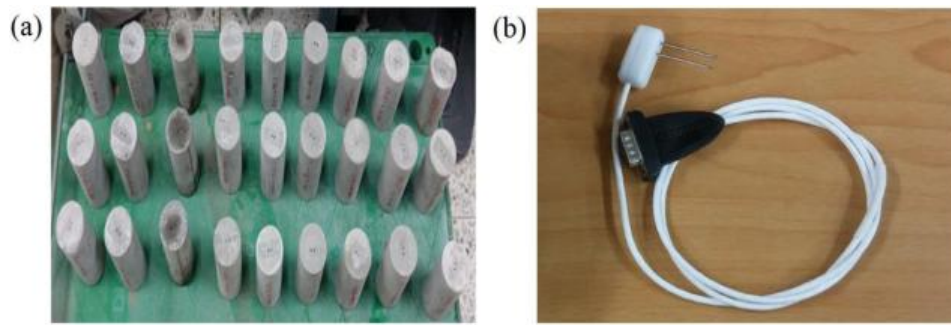


Fig. 3. (a) Prepared experimental specimens, (b) SH-1 sensor.

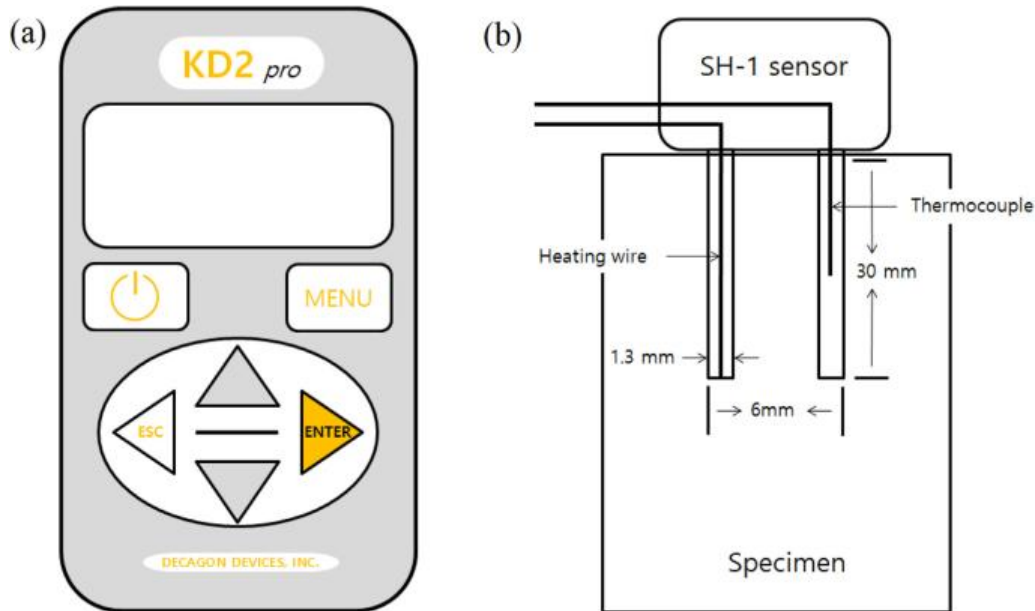


Fig. 4. Schematic representations of (a) KD2 pro and (b) SH-1 sensor.

prepared with NX length to diameter ratio (5 cm diameter \times 10 cm height) (Fig. 3(a)).

Due to the shape of the thermal property measurement sensor used in this investigation (Fig. 3(b)), the specimens were manufactured as follows: uncured cementitious grout was mixed and placed in the NX mold. After applying Vaseline to the pilot pin, which was the same size as the sensor, the pin was inserted into the specimen. The pin was removed after 24 h. Subsequently, the specimen was demolded and cured at room temperature for 28 days.

2.2. Measurement of thermal properties

The device used to measure thermal properties was a KD2-PRO (Decagon Manufacturing Co., Ltd.), which has an LCD display and a keypad (Fig. 4(a)). Either single- (KS-1, TR-1, RK-1) or double-needle sensors (SH-1) can be mounted onto a KD2-PRO. Single-needle sensors can measure only thermal conductivity and resistivity. However, a double-needle sensor can measure thermal conductivity, thermal resistivity, volumetric specific heat and thermal diffusivity. Therefore, in this study, the thermal properties of the specimens were measured using an SH-1 sensor. The specifications of the SH-1 sensor are shown in Table 2 [32].

The KD2-PRO measures the thermal properties of the medium using the transient line heat source method [32], and the measurement principles of the SH-1 sensor are as follows. Of the two

needles of an SH-1 sensor, one is a line-source heater, which is subjected to a heat pulse, and the other is a thermocouple, which is used to monitor the temperature (Fig. 4(b)). After inserting the SH-1 sensor into a medium, a heat pulse is applied to the heater and the temperature at the thermocouple is recorded as a function of time. The thermocouple's temperature response to the heat pulse is used to evaluate the thermal conductivity and thermal diffusivity simultaneously. The volumetric specific-heat constant is then determined based on these parameters [33].

The volumetric specific heat (c_v , J/m³·K) of a medium is defined as:

$$c_v = c_m \times \rho \quad (1)$$

where, c_m (J/kg·K) and ρ (kg/m³) are the specific-heat capacity and the wet-bulk density at the time of the volumetric-heat-capacity measurement, respectively.

As $\rho = \rho_d \times (1 + w_{act})$, the specific-heat capacity (c_m) of a medium is

$$c_m = \frac{c_v}{\rho_d \times (1 + w_{act})} \quad (2)$$

where, ρ_d (kg/m³) is the dry-bulk density and w_{act} is the moisture content at the moment of the volumetric-heat-capacity measurement. Moreover, w_{act} refers to the water-mass percentage filling of voids inside the specimen and is added to the equation as a multiplication factor of ρ_d .

Table 2
Specifications of the SH-1 sensor.

Size	Range	Accuracy	Measurable materials
–1.3 mm diameter × 30 mm length, 6-mm spacing	– 0.02 to 2.00 W/m·K (thermal conductivity) – 0.5 to 4 mJ/m ³ ·K (volumetric specific heat) – 0.1 to 1 mm ² /s (thermal diffusivity)	– ± 10% from 0.2–2 W/m·K (thermal conductivity) – ± 10% at conductivities above 0.1 W/m·K (volumetric specific heat) – ± 10% at conductivities above 0.1 W/m·K (thermal diffusivity)	– concrete, rock, moist soil, dry soil, powders, granular materials and other solids

Eq. (2) was used to calculate the specific-heat capacity (c_m) of the specimen [34].

To obtain the values of the saturated and dry bulk densities, which are required to calculate the specific-heat capacity and porosity of the specimens, their dry unit weights were measured after oven-drying the cured specimens at $105 \pm 2^\circ\text{C}$ for 2 days. Then, after water saturation by immersion for 5 days, their saturated unit weights and thermal properties were measured. To investigate the specimens' thermal properties under partially saturated conditions, one specimen of each mix proportion was selected at random. The selected specimens were then dried at room temperature ($22 \pm 2^\circ\text{C}$) and their thermal properties and weights were measured continuously for 30 days, by which time the measured values stopped varying significantly. When the thermal properties of the specimens were measured, thermal grease was applied to the sensor to provide optimal contact between the sensor and the specimen [32]. The thermal properties were evaluated under air-dried conditions by drying the other specimens for 30 days and measuring their thermal properties.

In this study, the changes in the moisture content of the specimens were represented by the degree of saturation

$$S = \frac{W_{act} - W_{dry}}{W_{sat} - W_{dry}} \quad (3)$$

where S is the degree of saturation, W_{act} is the specimen unit weight at the time of measurement (g), and W_{dry} and W_{sat} are the unit weights of the specimens under oven-dried and saturated conditions (g), respectively.

3. Results and discussion

3.1. Thermal properties under saturated and air-dried conditions

Previous experimental data were used to validate the experimental results. In a previous study, Kim et al. [25] investigated the thermal conductivity and specific-heat capacity of cementitious grouts under saturated and oven-dried conditions. Their grouts were prepared with the same mix proportions as those used in this study. Fig. 5(a,b) shows the thermal conductivity and specific-heat capacity of each specimen, measured under saturated conditions in the present study and in the previous study [25]. The results of this study are in good agreement with the previous experimental results [25]. Specifically, under saturated conditions, the thermal conductivity increased as the w/c ratio decreased and the s/c ratio increased, while the specific-heat capacity decreased. Moreover, the percentage differences in thermal conductivity and specific-heat capacity between the present and previous studies are small, at 1.23–9.57% and 0.34–7.55%, respectively. Therefore, the experimental results are reliable.

Table 3 summarizes the mean density and porosity of each specimen. As the w/c ratio decreased and the s/c ratio increased, the saturated and dry densities increased, while the porosity decreased. These results are consistent with those of a previous study [25]. Table 4 shows the mean thermal properties of each specimen, measured under saturated and air-dried conditions. When compared with the results obtained under saturated conditions,

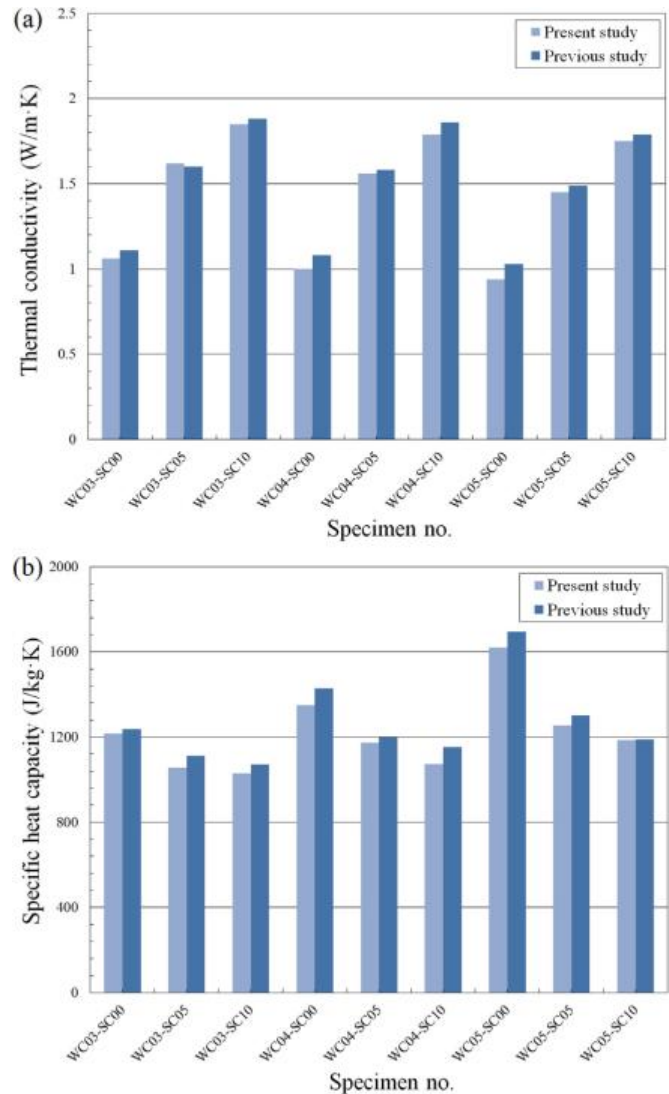


Fig. 5. Comparison between the results of the present study and a previous study: (a) thermal conductivity, (b) specific-heat capacity.

the thermal conductivity under the air-dried conditions decreased by 15.56–38.30%, and the specific-heat capacity by 11.79–22.34%. Moreover, the thermal properties diminished more as the w/c ratio increased and the s/c ratio decreased. This was due to the influence of porosity. Fig. 6 (a,b) shows the relationship between porosity and the reduction rate of the thermal properties. Here, the porosity represents how much of a specimen's interconnected void was accessible to water or air, and the reduction rate of the thermal properties was calculated as:

$$\text{Reduction rate (\%)} = \frac{(TP_d - TP_s)}{TP_s} \times 100 \quad (4)$$

Table 3
Density and porosity of specimens.

Specimen no.	Saturated density (kg/m ³)	Dry density (kg/m ³)	Porosity (%)
WC03-SC00	2134	1864	26.85
WC03-SC05	2229	2028	16.54
WC03-SC10	2255	2128	13.69
WC04-SC00	2043	1694	40.22
WC04-SC05	2212	1981	28.52
WC04-SC10	2227	2047	20.19
WC05-SC00	1954	1555	45.09
WC05-SC05	2092	1793	35.01
WC05-SC10	2211	1984	24.53

Table 4
Thermal properties of specimens measured under saturated and air-dried conditions.

Specimen no.	Thermal conductivity (W/m.K)			Specific-heat capacity (J/kg.K)		
	Saturated condition	Air-dried condition	Reduction rate (%)	Saturated condition	Air-dried condition	Reduction rate (%)
WC03-SC00	1.06	0.79	25.75	1216	1009	17.03
WC03-SC05	1.62	1.28	20.99	1056	917	13.12
WC03-SC10	1.87	1.58	15.56	1030	909	11.79
WC04-SC00	1.00	0.69	31.20	1350	1070	20.78
WC04-SC05	1.56	1.19	23.97	1173	949	19.11
WC04-SC10	1.82	1.50	17.53	1073	942	12.18
WC05-SC00	0.94	0.58	38.30	1621	1259	22.34
WC05-SC05	1.45	1.10	24.48	1256	988	21.34
WC05-SC10	1.79	1.40	21.84	1185	983	17.03

Table 5
Linear regression equations and coefficients between the thermal conductivity and degree of saturation for each specimen.

Specimen no.	Liner regression equation	R ²
WC03-SC00	TC = 0.42S + 0.64	0.97
WC03-SC05	TC = 0.51S + 1.09	0.98
WC03-SC10	TC = 0.52S + 1.37	0.98
WC04-SC00	TC = 0.41S + 0.59	0.97
WC04-SC05	TC = 0.49S + 1.06	0.98
WC04-SC10	TC = 0.51S + 1.38	0.97
WC05-SC00	TC = 0.40S + 0.54	0.99
WC05-SC05	TC = 0.46S + 0.99	0.98
WC05-SC10	TC = 0.48S + 1.32	0.96

Table 6
Linear regression equations and coefficients between the specific-heat capacity and degree of saturation of each specimen.

Specimen no.	Liner regression equation	R ²
WC03-SC00	SHC = 308S + 890	0.96
WC03-SC05	SHC = 137S + 866	0.95
WC03-SC10	SHC = 68S + 903	0.80
WC04-SC00	SHC = 320S + 974	0.96
WC04-SC05	SHC = 241S + 886	0.96
WC04-SC10	SHC = 123S + 913	0.78
WC05-SC00	SHC = 467S + 1137	0.87
WC05-SC05	SHC = 248S + 931	0.93
WC05-SC10	SHC = 219S + 942	0.87

where TP_d and TP_s are the mean thermal conductivity or specific-heat capacity of each specimen under air-dried and saturated conditions, respectively.

As shown in Fig. 6 (a,b), the higher the porosity of the specimen, the higher the reduction rate of the thermal properties. Under saturated conditions, the voids in the specimen filled with water, while under air-dried conditions, the voids were filled mainly with air. Water has a higher thermal conductivity and specific-heat capacity than air: 0.6 W/m.K and 4182 J/kg.K versus 0.025 W/m.K and 1005 J/kg.K at 20 °C, respectively [35,36]. Therefore, the higher the porosity of the specimen, the more water or air can fill the void, thus increasing the reduction rate of the thermal properties under both saturated and air-dried conditions.

3.2. Thermal properties under partially saturated conditions

Fig. 7 shows the relationship between the thermal conductivity and degree of saturation of the specimens. Table 5 lists the linear regression equations for the thermal conductivity (TC, W/m.K) and degree of saturation (S) of the specimens with the coefficient of determination, R². The thermal conductivity decreased linearly as the degree of saturation decreased. With equal degrees of saturation, the thermal conductivity increased as the w/c ratio decreased from 0.5 to 0.3 and the s/c ratio increased from 0 to 1. Moreover, the thermal conductivity decreased more steeply with decreasing

saturation. This was due to the reduction in porosity caused by the increase in the s/c ratio or the decrease in the w/c ratio. As mentioned above, water has a significant influence on the thermal properties of a medium. Moreover, the lower the porosity, the less water is retained within the voids. In other words, the lower the porosity, the lower the moisture content with the same degree of saturation. Therefore, the lower the porosity of the specimen, the more steeply the thermal conductivity decreases. Also, as shown in Fig. 7, under partially saturated conditions the increase in thermal conductivity caused by the increase in the s/c ratio was much more pronounced than that caused by the decrease in the w/c ratio. This indicates that increasing the s/c ratio has a greater effect on the increase in thermal conductivity of a cementitious grout than increasing the w/c ratio. This effect was observed over the whole range of saturation values tested.

Fig. 8 shows the relationship between the specific-heat capacity and degree of saturation of the specimens. Table 6 summarizes the linear regression equations of the specific-heat capacity (SHC, J/kg.K) and degree of saturation (S) of the specimens with the coefficient of determination, R². The specific-heat capacity decreased linearly with decreasing saturation. In general, the specific-heat capacity at equal degrees of saturation was higher when the w/c ratio increased from 0.3 to 0.5 and the s/c ratio decreased from 1 to 0. Moreover, the specific-heat capacity decreased more steeply with decreasing saturation. However, the changes in specific-heat

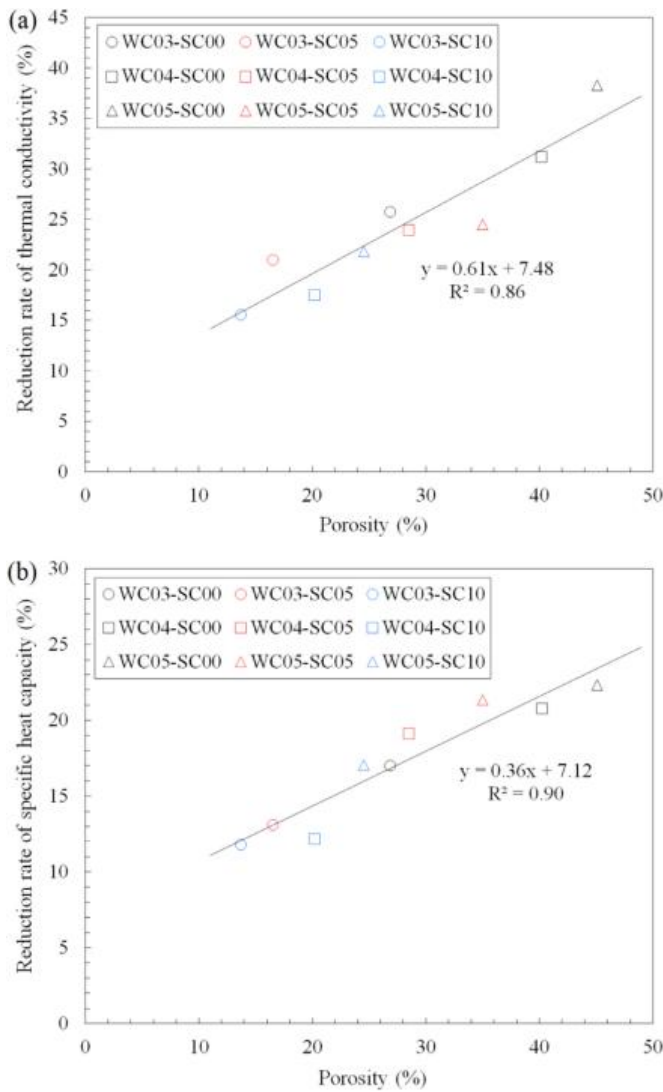


Fig. 6. Relationship between the porosity and reduction rate of the thermal properties: (a) thermal conductivity, (b) specific-heat capacity.

capacity caused by varying the mixing ratio were not as clearly distinguished as the changes in thermal conductivity, as shown in Fig. 7. Particularly with decreasing w/c ratios and increasing s/c ratios, the difference in specific-heat capacity at equal degrees of saturation decreased. That is, when comparing WC05-SC05 with WC05-SC10, WC04-SC05 with WC04-SC10, and WC03-SC05 with WC03-SC10, the differences in specific-heat capacity were small. Moreover, as the degree of saturation declined, this difference almost disappeared, due to the influence of the water's high specific-heat capacity and the decline in the porosity caused by the increase in the s/c ratio or the decrease in the w/c ratio. The specific-heat capacity of water is higher than that of any other common material. Moreover, the higher the porosity of the specimen, the more voids there are for water to fill. Therefore, under partially saturated conditions, the specific-heat capacity of the cementitious grout was affected by the amount of water in the voids. Table 7 shows the linear regression relationship between the degree of saturation (S) of each specimen and the amount of water (AW, g) retained by the specimen at that degree of saturation. Fig. 9 shows the relationship between the gradient values in Tables 6 and 7. As shown in Fig. 9, the gradients are highly correlated. These results indicate that, under partially saturated conditions, the specific-heat capacity of cementitious grouts is

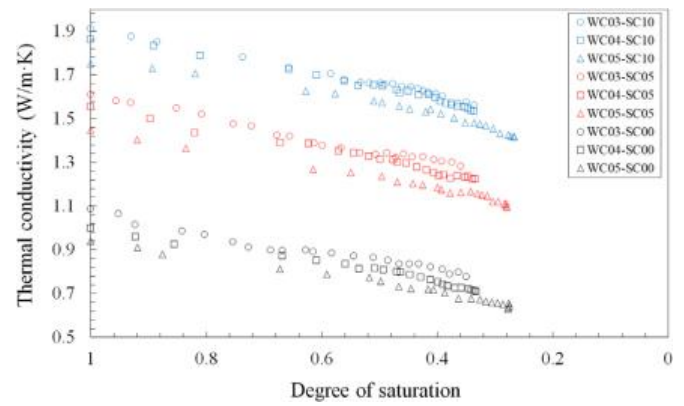


Fig. 7. Relationship between the thermal conductivity and degree of saturation of the specimens.

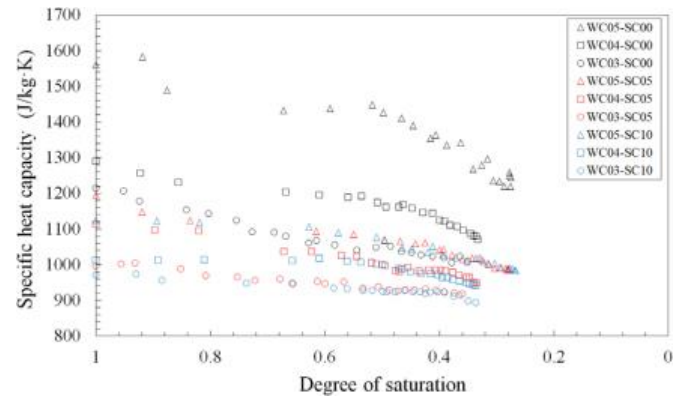


Fig. 8. Relationship between the specific-heat capacity and degree of saturation of the specimens.

Table 7

Linear regression equations and coefficients between the amount of retained water and the degree of saturation for each specimen.

Specimen no.	Linear regression equation	R ²
WC03-SC00	AW = 50.11S	1.00
WC03-SC05	AW = 38.57S	1.00
WC03-SC10	AW = 24.05S	1.00
WC04-SC00	AW = 62.80S	1.00
WC04-SC05	AW = 40.85S	1.00
WC04-SC10	AW = 32.17S	1.00
WC05-SC00	AW = 68.49S	1.00
WC05-SC05	AW = 54.31S	1.00
WC05-SC10	AW = 40.04S	1.00

significantly influenced by the amount of water retained within their voids.

3.3. Development of empirical equations for predicting thermal properties

In previous studies [37–40], cementitious grouts with various proportions of sand, which was used as an additive, were tested in actual sites. Therefore, if empirical equations are developed to predict the thermal properties of cementitious grout with various mixing ratios, they can be used for numerical analysis of the heat transmission and installation configurations of GSHPs. Hence, empirical equations to predict the thermal conductivity and specific-heat capacity of cementitious grouts with various mixing ratios under partially saturated conditions were derived based on the results presented in this paper.

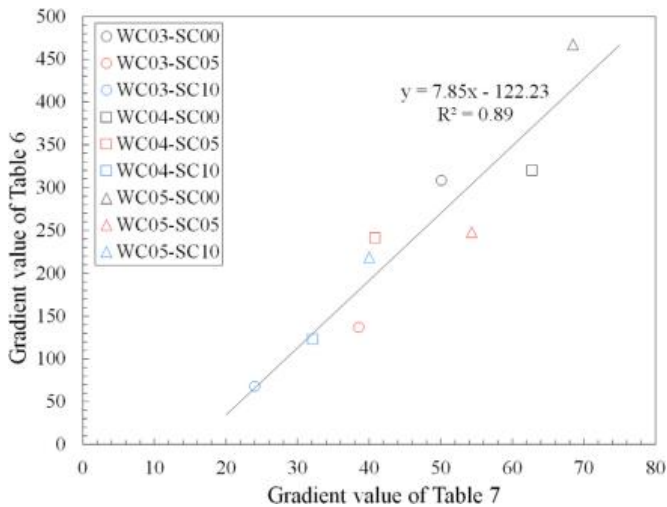


Fig. 9. Relationship between the gradient values in Tables 6 and 7.

In this study, the thermal conductivity and specific-heat capacity of cementitious grout decreased linearly with decreasing saturation. Also, as the w/c ratio decreased, and the s/c ratio increased, the thermal conductivity was higher with the same degree of saturation. The thermal conductivity decreased more steeply with decreasing saturation. However, the specific-heat capacity increased when the degree of saturation was held constant, but the w/c ratio increased, and the s/c ratio decreased. The specific-heat capacity decreased more steeply when the degree of saturation decreased. Therefore, a multiple regression analysis with thermal conductivity and specific-heat capacity as dependent variables was carried out, with the w/c ratio, s/c ratio, and degree of saturation as independent variables. The SPSS statistical package (IBM Corp., Armonk, NY, USA) was used for the multiple regression analysis and empirical equations were derived based on the results. The empirical equations derived from the multiple regression analysis are defined in Eqs. (5) and (6).

$$TC = -0.85 \times WC + 0.83 \times SC + 0.48 \times S + 0.91 \quad (\text{adj.}R^2 = 0.98) \quad (5)$$

$$SHC = 941 \times WC - 203 \times SC + 230 \times S + 667 \quad (\text{adj.}R^2 = 0.77) \quad (6)$$

where, TC, SHC, WC, SC, and S are the thermal conductivity (W/m.K), specific-heat capacity (J/kg.K), w/c ratio, s/c ratio, and degree of saturation, respectively.

Fig. 10 (a, b) shows the relationships of the measured thermal properties and predicted thermal properties calculated using the empirical equations. The deviation between the measured thermal properties and the predicted thermal properties is generally less than 10%. However, the empirical equation for the specific-heat capacity did not agree as well with the measurements results as that of the thermal conductivity. This was thought to be due to the influence of the specimens with the highest and lowest specific-heat capacities, i.e., WC05-SC00 and WC03-SC10, respectively. As shown in Fig. 9(b), as the specific-heat capacity of WC05-SC00 increased or the specific-heat capacity of WC03-SC10 decreased, the values derived from the plots representing the relationship between measured and predicted specific-heat capacities become negative, i.e., close to the -10% line, but the points for the other specimens are near the middle line of the graph, or positive, i.e., close to the $+10\%$ line. Therefore, the SH-1 sensor used in this study seems to be less accurate in the cases of small and large

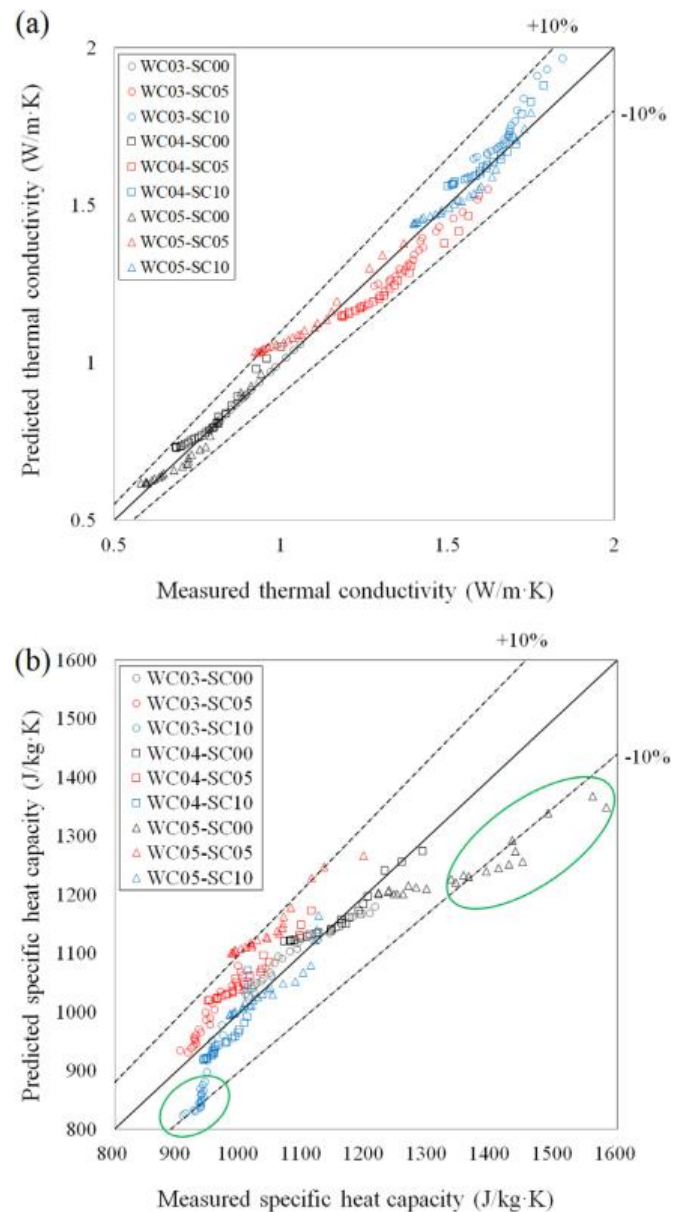


Fig. 10. (a, b). Relationships of the measured thermal properties and predicted thermal properties: (a) thermal conductivity, (b) specific-heat capacity.

specific-heat capacities, i.e., when the specific-heat capacity is less than 950 J/kg.K or greater than 1350 J/kg.K. However, additional studies should be carried out to investigate this issue, because other factors may be important.

4. Conclusions

In this study, the thermal properties of cementitious grouts used for vertical BHEs were measured under saturated, air-dried, and partially saturated conditions. The relationships of the mixing ratio of the cementitious grouts, degree of saturation, and thermal properties were also analyzed. The results were as follows:

- (1) Compared with the saturated condition, the thermal conductivity and specific-heat capacity of the cementitious grout under air-dried conditions decreased by 15.56–38.30% and 11.79–22.34%, respectively. Moreover, as the w/c ratio increased, and the s/c ratio decreased, the reductions in

thermal conductivity and specific-heat capacity increased. These effects were due to the influence of porosity.

- (2) Under partially saturated conditions, the thermal conductivity and specific-heat capacity of cementitious grout decreased linearly as the degree of saturation decreased. Also, as the w/c ratio decreased, and the s/c ratio increased, the thermal conductivity was higher with the same degree of saturation. Decreasing the degree of saturation caused a steeper decrease in the thermal conductivity. However, as the w/c ratio increased and the s/c ratio decreased, the specific-heat capacity was higher with the same degree of saturation. The specific-heat capacity decreased more steeply with decreasing saturation.
- (3) An increase in the s/c ratio had a greater effect on the increase in the thermal conductivity of the cementitious grout than did a reduction in the w/c ratio, and this effect was observed over the whole range of saturations. Also, due to the influence of the high specific-heat capacity of water, the specific-heat capacity of the cementitious grout was affected by the amount of water filling voids. This effect almost disappeared when the degree of saturation and porosity decreased.
- (4) Based on the findings of this study, empirical equations were derived to predict the thermal conductivity and specific-heat capacity of cementitious grout with various mixing ratios, which are as follows:

$$TC = -0.85 \times WC + 0.83 \times SC + 0.48 \times S + 0.91 (\text{adj.}R^2 = 0.98)$$

$$SHC = 941 \times WC - 203 \times SC + 230 \times S + 667 (\text{adj.}R^2 = 0.77)$$

These equations can be used as input parameters for numerical heat transmission analysis in further studies on vertical BHES. However, further study is required to investigate why the empirical equation for the specific-heat capacity was less well correlated with the measurement results.

Conflicts of interest

All authors certify that they have no affiliations with or involvement in any organization or entity with any financial interest (Such as honoraria; educational grants; participation in speakers' bureaus; membership, employment, consultancies, stock ownership, or other equity interest; and expert testimony or patent-licensing arrangements), or non-financial interest (such as personal or professional relationships, affiliations, knowledge or beliefs) in the subject matter or materials discussed in this manuscript.

Acknowledgement

This work was supported by the Nuclear Safety Research Program through the Korea Foundation Of Nuclear Safety (KoFONS) and granted financial resource from the Nuclear Safety and Security Commission (NSSC), Republic of Korea (no. 1705010). This research was also supported by Basic Science Research Program through the National Research Foundation of Korea (NRF) funded by the Ministry of Education (no. 2019R1A6A1A03033167).

References

- [1] L. Pérez, J. Ortiz, C. Pout, A review on buildings energy consumption information, *Energy Build.* 40 (2008) 394–398.
- [2] U.S. Energy Information Administration, Monthly and annual energy consumption, Online: <https://www.eia.gov/tools/faqs/faq.php?id=86&t=1>.
- [3] Environmental and Energy Study Institute, Buildings and climate change, Online: <https://www.eesi.org/files/climate.pdf>.
- [4] J. Seo, R. Ooka, J.T. Kim, Y. Nam, Optimization of the HVAC system design to minimize primary energy demand, *Energy Build.* 76 (2014) 102–108.
- [5] J. Wang, G. Huang, Y. Sun, X. Liu, Event-driven optimization of complex HVAC systems, *Energy Build.* 133 (2016) 79–87.
- [6] A. Ghahramani, S. Ahmadi Karvigh, B. Becerik-Gerber, HVAC system energy optimization using an adaptive hybrid metaheuristic, *Energy Build.* 152 (2017) 149–161.
- [7] J. Granderson, G. Lin, R. Singla, S. Fernandes, S. Touzani, Field evaluation of performance of HVAC optimization system in commercial buildings, *Energy Build.* 173 (2018) 577–586.
- [8] Y. Chen, L.K. Norford, H.W. Samuelson, A. Malkawi, Optimal control of HVAC and window systems for natural ventilation through reinforcement learning, *Energy Build.* 169 (2018) 195–205.
- [9] S. Wang, X. Liub, S. Gates, Comparative study of control strategies for hybrid GSHP system in the cooling dominated climate, *Energy Build.* 89 (2015) 222–230.
- [10] EPA, Space Conditioning: the Next Frontier 430-R-93-004 (4/93), Office of Air and Radiation, US Environmental Protection Agency, Washington, DC, 1993 Online: http://www.geoconnectionsinc.com/resources/EPA_spaceconditioning_the_next_frontier.html.
- [11] P. Cui, H. Yang, Z. Fang, Numerical analysis and experimental validation of heat transfer in ground heat exchangers in alternative operation modes, *Energy Build.* 40 (2008) 1060–1066.
- [12] P. Pascual-Muñoz, I. Indacochea-Vega, D. Zamora-Barraza, D. Castro-Fresno, Experimental analysis of enhanced cement-sand-based geothermal grouting materials, *Constr. Build. Mater.* 180 (2018) 481–488.
- [13] S. Park, D. Lee, H. Choi, K. Jung, H. Choi, Relative constructability and thermal performance of cast-in-place concrete energy pile: coil-type GHEX (ground heat exchanger), *Energy* 81 (2015) 56–66 *Energy* 8156–66.
- [14] M.L. Allan, Thermally Conductive Cementitious Grouts for Geothermal Heat Pumps, Upton, US—NY: FY 97, 1997 Progress Report, BNL-65129 Online: <https://www.osti.gov/servlets/purl/760977>.
- [15] C.P. Remund, J.T. Lund, Thermal enhancement of bentonite grouts for vertical GSHP system, *ASME* 29 (1993) 95–106.
- [16] A.M. Omer, Experimental investigation of the performance of a ground source heat pump system for buildings heating and cooling, *IJIMSEP* 4 (2016) 10–44 Online: <http://seahipaj.org/journals-ci/mar-2016/IJIMSEP/full/IJIMSEP-M-2-2016.pdf>.
- [17] C.H. Lee, K.J. Lee, H.S. Choi, H.P. Choi, Characteristics of thermally-enhanced bentonite grouts for geothermal heat exchanger in South Korea, *Sci. China Technol. Sci.* 53 (2011) 123–128.
- [18] A.J. Philippopoulos, M.L. Berndt, Influence of debonding in ground heat exchangers used with geothermal heat pumps, *Geothermics* 30 (2001) 527–545.
- [19] H. Javadi, S.S.M. Ajarostaghi, M.A. Rosen, M. Pourfallah, A comprehensive review of backfill materials and their effects on ground heat exchanger performance, *Sustainability* 10 (2018) 4486.
- [20] M.L. Allan, S.P. Kavanaugh, Thermal conductivity of cementitious grouts and impact on heat exchanger length design for ground source heat pumps, *HVAC&R Res.* 5 (2011) 85–96.
- [21] M.S. Park, S.H. Min, J.H. Lim, J.M. Choi, H.S. Choi, Applicability of cement-based grout for ground heat exchanger considering heating-cooling cycles, *Sci. China Technol. Sci.* 54 (2011) 1661–1667.
- [22] M.L. Allan, A.J. Philippopoulos, Properties and performance of thermally conductive cement-based grouts for geothermal heat pumps; Department of Applied Science, Brookhaven National Laboratory, Upton, US—NY: FY 99, 1999 Final Report, BNL-67006 Online: <https://www.osti.gov/servlets/purl/751116/>.
- [23] A.A. Alrtimi, M. Rouania, D.A.C. Manning, Thermal enhancement of PFA-based grout for geothermal heat exchangers, *Appl. Therm. Eng.* 2 (2013) 559–564.
- [24] C.J. Han, X. Yu, Sensitivity analysis of a vertical geothermal heat pump system, *Appl. Energy* 170 (2016) 148–160.
- [25] D. Kim, G. Kim, D. Kim, H. Baek, Experimental and numerical investigation of thermal properties of cement-based grouts used for vertical ground heat exchanger, *Renew. Energy* 112 (2017) 260–267.
- [26] L. Zhang, Z. Lei, Y. Liu, S. Hu, Analyses on soil temperature responses to intermittent heat rejection from BHES in soils with groundwater advection, *Energy Build.* 107 (2015) 355–365.
- [27] O.T. Farouki, Thermal Properties of soil, Series On Rock and Soil Mechanics, Trans Tech Publication, Germany, 1986.
- [28] J.L. Hanson, T.B. Edil, N. Yesiller, Thermal properties of high water content materials, geotechnics of high water content materials, *ASTM STP* 1374 (2000) 137–151 Online: https://digitalcommons.calpoly.edu/cenv_fac/258/.
- [29] P. Nagaraju, S. Roy, Effect of water saturation on rock thermal conductivity measurements, *Tectonophysics* 626 (2014) 137–143.
- [30] D. Kim, G. Kim, H. Baek, Thermal conductivities under unsaturated condition and mechanical properties of cement-based grout for vertical ground-heat exchangers in Korea-A case study, *Energy Build.* 122 (2016) 34–41.
- [31] D. Kim, G. Kim, H. Baek, Relationship between thermal conductivity and soil-water characteristic curve of pure bentonite-based grout, *Int. J. Heat Mass Transf.* 84 (2015) 1049–1055.
- [32] KD2 pro manual, Online: http://manuals.decagon.com/Manuals/13351_KD2%20Pro_Web.pdf.
- [33] R.J. Issa, K. Leitch, B. Chang, Experimental heat transfer study on green roofs in a semiarid climate during summer, *J. Constr. Eng.* 2015 (2015) 960538.
- [34] K.A. Alnefaie, N.H. Abu-Hamdeh, Specific heat and volumetric heat capacity of some saudian soils as affected by moisture and density, in: Proceedings of the 2013 International Conference on Mechanics, Fluids, Heat, Elasticity and Electromagnetic Fields, 2013, pp. 139–143. <http://www.inase.org/library/2013/venice/bypaper/MFHEEF/MFHEEF-21.pdf>.
- [35] Engineeringtoolbox, Online: http://www.engineeringtoolbox.com/specific-heat-capacity-d_391.html.

- [36] H. Hens, *Applied Building Physics: Boundary Conditions, Building Performance and Material Properties*, Wiley, Germany, 2010.
- [37] C. Lee, M. Park, B. Nguyen, B. Sohn, J.M. Choi, H. Choi, Performance evaluation of closed-loop vertical ground heat exchangers by conducting in-situ thermal response tests, *Renew. Energy* 42 (2012) 77–83.
- [38] W. Choi, R. Ooka, Effect of disturbance on thermal response test, part 2: numerical study of applicability and limitation of infinite line source model for interpretation under disturbance from outdoor environment, *Renew. Energy* 85 (2016) 1090–1105.
- [39] S. Yoon, S. Lee, G. Go, J. Xue, H. Park, D. Park, Thermal transfer behavior in two types of W-shape ground heat exchangers installed in multilayer soils, *Geomech. Eng.* 6 (2014) 79–98.
- [40] P. Hemmingway, M. Long, Interpretation of in situ and laboratory thermal measurements resulting in accurate thermogeological characterization, in: R.Q. Coutinho, P.W. Mayne (Eds.), *Geotechnical and Geophysical Site Characterization 4*, Taylor & Francis, London, 2012, pp. 1779–1787. <http://hdl.handle.net/10197/3942>.